NASA TECHNICAL NOTE

NASA TN D-2393

c. 1

LOAN COPY: RETI
AFWL (WLIL
KIRTLAND AFB, I

TECH LIBRARY KAFB, NM
0154923

NASA TN D-2393

LAMINAR SLIP FLOW HEAT TRANSFER IN A PARALLEL-PLATE CHANNEL OR A ROUND TUBE WITH UNIFORM WALL HEATING

by Robert M. Inman

Lewis Research Center
Cleveland, Ohio

NATIONAL AERONAUTICS AND SPACE ADMINISTRATION • WASHINGTON, D. C. • AUGUST 1964

ERRATA

NASA Technical Note D-2393

LAMINAR SLIP FLOW HEAT TRANSFER IN A PARALLEL-PLATE CHANNEL OR A ROUND TUBE WITH UNIFORM WALL HEATING

by Robert M. Inman
August 1964

Page 4, lines 2 and 18: The equation number should be (69) instead of (68).

Page 13: In the sentence preceding equation (36), the equation number should be (33) instead of (35).

Page 17, equation (45): The quantity $\left(\frac{3}{8}\right)^{1/2}$ should be $\left(\frac{3}{2}\right)^{1/2}$.

Page 18, equation (51): The quantity 8α should be 16α.

Page 19, equation (53): The quantity $\text{arc sin}\,\frac{1 - 2\eta}{(1 + 4\alpha)^{1/2}} - \text{arc sin}\,\frac{1}{(1 + 4\alpha)^{1/2}}$

should be enclosed in parentheses.

Page 19: In the sentence following equation (53), the equation number should be (52) instead of (53).

Page 31: Equation (83) should read

$$\tilde{I} \equiv \int_0^{\omega} \left[2f(\omega)\right]^{1/2} d\omega = \left[\omega(1 - \omega^2 + 4\alpha)^{1/2} + (1 + 4\alpha)\text{arc sin}\,\frac{\omega}{(1 + 4\alpha)^{1/2}}\right] \Big/ (1 + 8\alpha)^{1/2}$$

Page 31: In the sentence following equation (83), the reference numbers should be 1 and 3 instead of 1 and 4.

NASA-Langley, 1965

Issued 2-15-65

TECH LIBRARY KAFB, NM

0154923

LAMINAR SLIP FLOW HEAT TRANSFER IN A PARALLEL-PLATE CHANNEL OR A ROUND TUBE WITH UNIFORM WALL HEATING

By Robert M. Inman

Lewis Research Center
Cleveland, Ohio

NATIONAL AERONAUTICS AND SPACE ADMINISTRATION

For sale by the Office of Technical Services, Department of Commerce,
Washington, D.C. 20230 -- Price $1.00

LAMINAR SLIP FLOW HEAT TRANSFER IN A PARALLEL-PLATE CHANNEL OR A ROUND TUBE WITH UNIFORM WALL HEATING

by Robert M. Inman

Lewis Research Center

SUMMARY

An analysis has been made to determine the effects of low-density phenomena on the heat-transfer characteristics for laminar flow in a parallel-plate channel or in a circular tube with uniform wall heat flux. Consideration is given to the slip-flow regime wherein the major rarefaction effects are displayed as velocity and temperature jumps at the conduit walls. The results obtained apply along the entire length of the conduit, that is, in the thermal entrance region as well as far downstream. The solutions contain a series expansion, and analytical expressions for the complete set of eigenvalues and eigenfunctions for this problem are presented. The results give the wall temperatures, Nusselt numbers, and thermal entrance lengths for the conduits for various values of the rarefaction parameters. The results indicate that the slip-flow Nusselt numbers are lower than those for continuum flow at all axial locations along the conduits, and also that the thermal entrance length is decreased with increasing gas rarefaction for either the parallel-plate channel or the circular tube. Extension of the results is made or indicated to include the effects of shear work at the wall, modified temperature jump, and thermal creep velocity.

INTRODUCTION

In recent years, under the impetus of space flight, considerable interest has developed in the study of the fluid-flow and heat-transfer characteristics of rarefied gases. Most of the investigations have been concerned with external aerodynamic situations. Only very recently has attention been directed to the problem of heat transfer to rarefied gas flow in conduits, in particular, to forced-convection heat transfer. The corresponding problem for continuum flow has, of course, been the subject of much analysis and experimentation, and it is now possible to predict the heat-transfer performance for laminar continuum flow in a parallel-plate channel or in a circular tube with arbitrary axial wall temperature (refs. 1 and 2) or axial wall heat flux (refs. 3 to 7).

Of particular interest in internal, rarefied gas-flow studies has been the problem of laminar heat transfer in conduits under slip-flow conditions (ref. 8). The essential simplifications introduced in these investigations to obtain analytical solutions are fully established temperature profiles and fully developed velocity distributions.

The present investigation is concerned with the more general problem of determining the heat-transfer characteristics along the entire length of the conduit, that is, in the thermal entrance region as well as far downstream, for laminar slip flow in a parallel-plate channel or in a circular tube with uniform wall heat flux. It should be mentioned at the outset, however, that one of the simplifications introduced to obtain analytical solutions to the previously mentioned problem is such that direct application of the results may not be possible. In particular, a fully developed velocity profile that is unchanging along the conduit length is assumed. While this is a case that is believed physically reasonable in that portion of the conduit where the fully developed heat-transfer condition is attained for uniform wall heat flux (ref. 8), it is perhaps not a good approximation in the thermal entrance region, where the effect of thermal creep may not be strictly negligible. Nevertheless, it is hoped that the understanding gained will lead toward the solution of a more realistic problem wherein the thermal creep effect is included.

In the section FLOW IN A PARALLEL-PLATE CHANNEL there is considered in some detail the problem of slip flow of a rarefied gas in a parallel-plate channel with uniform wall heat flux at one or at both walls. Both heating arrangements are frequently encountered in practical applications. The problem of slip flow in a circular tube with uniform wall heat flux is taken up in the section FLOW IN A CIRCULAR TUBE. In the final section of the investigation, modification of the heat-transfer results will be made and/or discussed to account for such effects as wall shear work, modified temperature jump, and thermal creep velocity.

SYMBOLS

A, B integration constants defined on pp. 17 and 19, $[f(0)]^{1/4}/2$

a accommodation coefficient

C_m coefficient in series for temperature distribution in parallel-plate channel

C_n coefficient in series for temperature distribution in circular tube

C_p specific heat at constant pressure

D_m coefficient defined by eq. (51) or (58)

D_n coefficient defined by eq. (89)

D_T thermal diameter, $8L/\sigma$

d	tube diameter, $2r_0$
E,F	constants defined by eqs. (47) and (56), respectively
$f(\eta)$	dimensionless velocity for parallel-plate channel, $u(\eta)/\bar{u}$
$f(\omega)$	dimensionless velocity for circular tube, $u(\omega)/\bar{u}$
$G(\eta)$	transverse temperature distribution in fully developed region for parallel-plate channel
g	specular reflection coefficient
$H(\omega)$	transverse temperature distribution in fully developed region for circular tube
h	heat-transfer coefficient, $q/(t_w - t_b)$
$I_1, \tilde{I}_1$	value of definite integral, eq. (46) or (55) for parallel-plate channel, eq. (85) for round tube
$\mathcal{I}$	value of indefinite integral, eq. (53)
J_0, J_1	Bessel functions of first kind
L	half distance between plates
l	mean free path
M,N	constant defined by eqs. (86) and (87), respectively
Nu	Nusselt number, hD_T/k or hd/k
Pr	Prandtl number, $\mu C_p/k$
p	static pressure
q	rate of heat flux per unit area from wall to fluid
q^*	shear work at wall, defined by eq. (91)
R	transverse or radial distribution function
Re	Reynolds number, $2\rho\bar{u}L/\mu$ for parallel-plate channel, $\rho\bar{u}d/\mu$ for circular tube
$R'(1)$	slope of $R(\eta)$ or $R(\omega)$ at wall
R_g	gas constant

R_m	eigenfunctions of eq. (23) for parallel-plate channel
R_n	eigenfunctions of eq. (68) for circular tube
r	radial coordinate
r_0	tube radius
t	temperature
t_g	gas temperature adjacent to wall
u	velocity
x	axial coordinate
y	transverse coordinate
α	dimensionless velocity slip coefficient, $\xi_u/2L$ or ξ_u/d
β_m	$\lambda_m^{1/2} I_1$ or $\lambda_m^{1/2} \mathcal{J}_1$
β_n	$\lambda_n \tilde{I}_1$
γ	ratio of specific heats
ζ	dimensionless coordinate, $x/2L$ or x/r_0
η	dimensionless coordinate, $\sigma y/2L$
κ	gas thermal conductivity
λ_m	eigenvalues of eq. (23) for parallel-plate channel
λ_n	eigenvalues of eq. (68) for round tube
μ	absolute viscosity
ξ_t	temperature-jump coefficient
ξ_u	velocity-slip coefficient
ρ	gas density
σ	symmetry number
φ	rarefaction parameter, $\mu\sqrt{R_g t}/2pL$ or $\mu\sqrt{R_g t}/pd$
ψ	dimensionless quantity, $RePr/\sigma^2$ for parallel-plate channel, $RePr/4$ for circular tube
ω	dimensionless coordinate, r/r_0

Subscripts:

b	bulk condition of gas
C	centerline
d	fully developed region
d, c	fully developed region for continuum flow
e	entrance region
i	gas entering channel, $x = 0$
s	slip condition at wall
w	wall
0	heated section entrance, $x = 0$

Superscript:

$(\bar{\ })$	average value

FLOW IN A PARALLEL-PLATE CHANNEL

The coordinate systems for the problems under study are shown in figure 1.

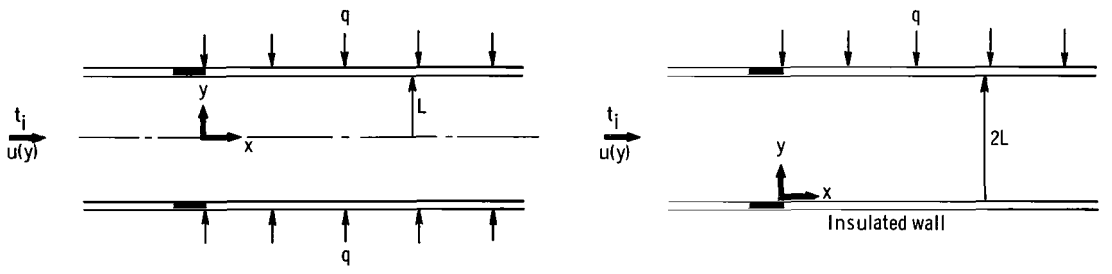

(a) Symmetry number, 2.

(b) Symmetry number, 1.

Figure 1. - Physical model and coordinate system for parallel-plate channel.

A slightly rarefied gas flows in the positive x-direction with a fully established velocity profile. Up to a point $x = 0$ the flow is isothermal at temperature t_i. After this point a uniform wall heat flux is applied. It is desired to determine the temperature distribution and the variation in the heat-transfer coefficient along the entire length of the channel, that is, in the thermal entrance region as well as in the fully developed region.

It is convenient to place the plane $y = 0$ at the plane of symmetry, that is, at the middle of the duct in case of heating at both walls at $y = \pm L$ (fig. 1(a)) and at the insulated wall in case of heating from one side at $y = 2L$

(fig. 1(b)).

Both cases are included in the following development by defining a symmetry number σ, which is also the number of heating surfaces (ref. 4).

The velocity problem is examined first, since the heat-transfer analysis requires a prior knowledge of the velocity characteristics.

Velocity Problem

The flow is assumed to be governed by the continuum form of the momentum conservation equation, which, for fully developed incompressible duct flow, reduces to

$$\frac{1}{\mu}\frac{\partial p}{\partial x} = \frac{\partial^2 u}{\partial y^2} \tag{1}$$

The slip-flow boundary condition, which permits a slip velocity u_s at the duct walls ($y = \pm L$, $\sigma = 2$; $y = 0$, $2L$, $\sigma = 1$), is written as (ref. 9)

$$\left.\begin{aligned} u(-L) &= u_s = \xi_u\left(\frac{\partial u}{\partial y}\right)_{y=-L} \\ u(+L) &= u_s = -\xi_u\left(\frac{\partial u}{\partial y}\right)_{y=+L} \end{aligned}\right\}\sigma = 2 \tag{2}$$

$$\left.\begin{aligned} u(0) &= u_s = \xi_u\left(\frac{\partial u}{\partial y}\right)_{y=0} \\ u(2L) &= u_s = -\xi_u\left(\frac{\partial u}{\partial y}\right)_{y=2L} \end{aligned}\right\}\sigma = 1 \tag{3}$$

The slip coefficient ξ_u is given by the expression (ref. 9)

$$\xi_u = \frac{2 - g}{g}\, l \tag{4}$$

where l is the mean free path and g is the specular reflection coefficient.

The solutions for the velocity distribution, slip velocity, and average velocity are found to be

$$\left.\begin{aligned} u(\eta) &= -\frac{L^2}{2\mu}\frac{dp}{dx}(1-\eta^2) + u_s \\ u_s &= -\frac{L^2}{\mu}\frac{dp}{dx}\frac{\xi_u}{L} \\ \bar{u} &= -\frac{L^2}{3\mu}\frac{dp}{dx}\left(1 + 3\frac{\xi_u}{L}\right) \end{aligned}\right\} \sigma = 2 \tag{5}$$

$$\left.\begin{aligned} u(\eta) &= -\frac{2L^2}{\mu}\frac{dp}{dx}(\eta-\eta^2) + u_s \\ u_s &= -\frac{2L^2}{\mu}\frac{dp}{dx}\frac{\xi_u}{2L} \\ \bar{u} &= -\frac{L^2}{3\mu}\frac{dp}{dx}\left(1 + 6\frac{\xi_u}{2L}\right) \end{aligned}\right\} \sigma = 1 \tag{6}$$

From these equations, dimensionless velocity profiles $u(\eta)/\bar{u}$, which will prove to be of importance in the heat-transfer problem, can be obtained:

$$f(\eta) = \frac{\frac{3}{2}(1-\eta^2+4\alpha)}{1+6\alpha} \qquad \sigma = 2 \tag{7}$$

$$f(\eta) = \frac{6(\eta-\eta^2+\alpha)}{1+6\alpha} \qquad \sigma = 1 \tag{8}$$

where $\alpha \equiv \xi_u/2L$. The relation between the average velocity and the slip velocity is easily obtained as

$$\frac{u_s}{\bar{u}} = \frac{6\alpha}{1+6\alpha} \qquad \sigma = 1,2 \tag{9}$$

Now that the fully developed velocity distributions have been determined, the solution of the heat-transfer problem is undertaken.

Energy Equation

The starting point of the analysis is the differential equation for convective heat transfer in the parallel-plate channel flow with fully established velocity profile. With the gas properties assumed constant, the heat conduction in the flow direction compared to that in the transverse y-direction assumed negligible, and the viscous dissipation assumed negligible, the equation can be written in the form

$$\rho C_p u \frac{\partial t}{\partial x} = \kappa \frac{\partial^2 t}{\partial y^2} \tag{10}$$

Equation (10) written in terms of dimensionless variables becomes

$$\psi f(\eta) \frac{\partial t}{\partial \zeta} = \frac{\partial^2 t}{\partial \eta^2} \tag{11}$$

The boundary conditions are as follows:

Specified wall heat flux:

$$\frac{\partial t}{\partial \eta} = \frac{2L}{\sigma} \frac{q}{\kappa} \quad \text{at} \quad \eta = 1, \; x \geq 0$$

Symmetry:

$$\frac{\partial t}{\partial \eta} = 0 \quad \text{at} \quad \eta = 0$$

Specified entrance temperature:

$$t = t_i \quad \text{at} \quad x = 0$$

Fully Developed Solution

When the wall heat flux is uniform, it is known that for very large values of x there is a fully developed thermal situation characterized by a linear rise in the temperature at all points in the cross section along the channel; that is,

$$\frac{\partial t_d}{\partial x} = \frac{\sigma q}{\mathrm{RePr}\kappa} \qquad \sigma = 2,1 \tag{12}$$

Equation (12) can be written alternatively as

$$\frac{t_d - t_i}{\frac{2L}{\sigma} \frac{q}{\kappa}} = \frac{\sigma^2 \frac{x}{2L}}{\mathrm{RePr}} + G(\eta) \tag{13}$$

The temperature t_d must satisfy equation (11); that is,

$$\psi f(\eta) \frac{\partial t_d}{\partial \zeta} = \frac{\partial^2 t_d}{\partial \eta^2} \tag{14}$$

When equation (13) is substituted into equation (14), the governing equation for $G(\eta)$ is

$$\frac{d^2G}{d\eta^2} = f(\eta) \tag{15}$$

The boundary conditions on $G(\eta)$ are determined from the conditions

$$\left.\begin{aligned} \left(\frac{dt_d}{d\eta}\right)_{\eta=0} &= 0 \\ \left(\frac{dt_d}{d\eta}\right)_{\eta=1} &= \frac{2L}{\sigma}\frac{q}{\kappa} \end{aligned}\right\} \tag{16}$$

so that

$$\left.\begin{aligned} \left(\frac{dG}{d\eta}\right)_{\eta=0} &= 0 \\ \left(\frac{dG}{d\eta}\right)_{\eta=1} &= 1 \end{aligned}\right\} \tag{17a}$$

Consideration of an overall energy balance on the fluid for the length of channel from 0 to x produces the additional condition on $G(\eta)$:

$$\left.\begin{aligned} \int_{-1}^{1} G(\eta)f(\eta)d\eta &= 0 \qquad \sigma = 2 \\ \int_{0}^{1} G(\eta)f(\eta)d\eta &= 0 \qquad \sigma = 1 \end{aligned}\right\} \tag{17b}$$

Equations (15), (17a), and (17b) are sufficient to determine the function $G(\eta)$. A different function is obtained for each value of σ. The function $G(\eta)$ for each case is

$$G(\eta) = \left[\frac{3}{4}\eta^2 - \frac{1}{8}\eta^4 - \frac{39}{280}\right] + \left[-\frac{1}{4}\eta^2 + \frac{1}{8}\eta^4 - \frac{13}{280}\right]\frac{u_s}{\bar{u}} + \left[\frac{2}{105}\right]\left(\frac{u_s}{\bar{u}}\right)^2 \qquad \sigma = 2 \tag{18a}$$

$$G(\eta) = \left[\eta^3 - \frac{1}{2}\eta^4 - \frac{9}{70}\right] + \left[\frac{1}{2}\eta^4 - \eta^3 + \frac{1}{2}\eta^2 - \frac{3}{70}\right]\frac{u_s}{\bar{u}} + \left[\frac{1}{210}\right]\left(\frac{u_s}{\bar{u}}\right)^2 \qquad \sigma = 1 \tag{18b}$$

The first quantity in brackets on the right side of equations (18a) and (18b) represents the usual transverse temperature distribution for continuum flow conditions, while the second and third quantities in brackets are connected with one effect of gas rarefaction, namely, that of velocity jump.

Entrance Region

To determine the solution in the entrance region it is convenient to define a difference temperature t_e as

$$t_e(\zeta,\eta) = t(\zeta,\eta) - t_d(\zeta,\eta) \tag{19}$$

Then t_e must satisfy the relation

$$\psi f(\eta) \frac{\partial t_e}{\partial \zeta} = \frac{\partial^2 t_e}{\partial \eta^2} \tag{20}$$

with boundary conditions

$$\frac{\partial t_e}{\partial \eta} = 0 \quad \text{at} \quad \eta = 0 \quad \text{and} \quad \eta = 1 \tag{21}$$

The condition at $x = 0$ will be discussed shortly.

The solution of equation (20) that will satisfy equation (21) can be found by using a product solution that leads to a separation of variables. This solution will have the form

$$\frac{t_e}{\frac{2L}{\sigma}\frac{q}{K}} = \sum_{m=1}^{\infty} C_m R_m(\eta) \exp\left(\frac{-\sigma^2 \lambda_m \frac{x}{2L}}{RePr}\right) \tag{22}$$

where λ_m and R_m are, respectively, the eigenvalues and eigenfunctions of the Sturm-Liouville problem:

$$\left.\begin{aligned} &\frac{d^2R}{d\eta^2} + \lambda f(\eta) R = 0 \\ &\frac{dR}{d\eta} = 0 \quad \text{at} \quad \eta = 0 \quad \text{and} \quad \eta = 1 \end{aligned}\right\} \sigma = 2,1 \tag{23}$$

The coefficients C_m in equation (22) are determined in the following way. When the boundary condition is applied at the entrance to the heated section $x = 0$,

$$t_e(0,\eta) = t_i - t_d(0,\eta)$$

Combining this result with equation (13) yields

$$\frac{t_e(0,\eta)}{\frac{2L}{\sigma}\frac{q}{K}} = -G(\eta) = \sum_{m=1}^{\infty} C_m R_m(\eta) \tag{24}$$

This result together with the orthogonality property of the eigenfunctions leads to

$$C_m = -\frac{\int_0^1 G(\eta)f(\eta)R_m(\eta)d\eta}{\int_0^1 f(\eta)R_m^2(\eta)d\eta}$$

$$= \frac{\int_0^1 G(\eta)f(\eta)R_m(\eta)d\eta}{\left[R(\eta)\ \frac{\partial^2 R}{\partial\eta\ \partial\lambda}\right]_{\eta=1,\ \lambda=\lambda_m}} \qquad \sigma = 2,1 \tag{25}$$

The integral in equation (25) can be evaluated by substituting $G(\eta)$ from equation (18a) or (18b) and $f(\eta)$ from equation (7) or (8), integrating by parts, and utilizing equation (23). The final result is identical for both cases:

$$C_m = \frac{1}{\left(\lambda\ \frac{\partial^2 R}{\partial\eta\ \partial\lambda}\right)_{\eta=1,\ \lambda=\lambda_m}} \qquad \sigma = 2,1 \tag{26}$$

This result clearly suggests that an analytical solution for the coefficients C_m is possible if expressions for the eigenvalues and eigenfunctions of equation (23) can be obtained. This possibility will be considered shortly.

The complete solution for the temperature that applies in both the entrance and the fully developed regions is found by adding the solutions for t_d and t_e to give

$$\frac{t - t_i}{\frac{2L}{\sigma}\ \frac{q}{K}} = \frac{\sigma^2\ \frac{x}{2L}}{RePr} + G(\eta) + \sum_{m=1}^{\infty} C_m R_m(\eta)\exp\left(\frac{-\sigma^2\lambda_m\ \frac{x}{2L}}{RePr}\right) \tag{27}$$

A result of practical interest is the longitudinal variation of wall temperature t_w corresponding to a uniform wall heat flux. Before the wall temperature variation can be determined, however, it is necessary to consider another effect of gas rarefaction that enters through the thermal boundary condition at the wall, which permits a jump between the surface temperature t_w and the adjacent gas temperature t_g (ref. 9):

$$t_g - t_w = -\xi_t\left(\frac{\partial t}{\partial y}\right)_{y=2L/\sigma} \tag{28}$$

where ξ_t represents a temperature-jump coefficient related to other properties of the system by

$$\xi_t = \frac{2 - a}{a} \frac{2\gamma}{\gamma + 1} \frac{l}{Pr} \tag{29}$$

For uniform wall heat flux,

$$\left(\frac{\partial t}{\partial y}\right)_{y=2L/\sigma} = \left(\frac{\partial t_d}{\partial y} + \frac{\partial t_e}{\partial y}\right)_{y=2L/\sigma} = \frac{q}{K}$$

so that the temperature jump at the wall can be written

$$t_g - t_w = - \frac{2L}{\sigma} \frac{q}{K} \frac{\sigma \xi_t}{2L} \tag{30}$$

Setting $\eta = 1$ in equation (27) and combining the result with equation (30) yield

$$\frac{t_w - t_i}{\frac{2L}{\sigma} \frac{q}{K}} = \frac{\sigma^2 \frac{x}{2L}}{RePr} + G(1) + \frac{\sigma \xi_t}{2L} + \sum_{m=1}^{\infty} C_m R_m(1) \exp\left(\frac{-\sigma^2 \lambda_m \frac{x}{2L}}{RePr}\right) \tag{31}$$

Another form of this equation is obtained by introducing the bulk temperature $t_b(x)$. For a uniform wall heat flux, the bulk temperature is given by

$$t_b = t_i + \sigma^2 \frac{\frac{2L}{\sigma} \frac{q}{K} \frac{x}{2L}}{RePr} \tag{32}$$

Combining equations (31) and (32) yields

$$\frac{t_w - t_b}{\frac{2L}{\sigma} \frac{q}{K}} = G(1) + \frac{\sigma \xi_t}{2L} + \sum_{m=1}^{\infty} C_m R_m(1) \exp\left(\frac{-\sigma^2 \lambda_m \frac{x}{2L}}{RePr}\right) \tag{33}$$

Then, for the fully developed situation,

$$\frac{(t_w - t_b)_d}{\frac{2L}{\sigma} \frac{q}{K}} = G(1) + \frac{\sigma \xi_t}{2L} \tag{34}$$

Dividing equation (33) by (34) yields the important ratio

$$\frac{t_w - t_b}{(t_w - t_b)_d} = \frac{G(1) + \frac{\sigma\xi_t}{2L} + \sum_{m=1}^{\infty} C_m R_m(1) \exp\left(\frac{-\sigma^2 \lambda_m \frac{x}{2L}}{RePr}\right)}{G(1) + \frac{\sigma\xi_t}{2L}} \tag{35}$$

Equation (35) can be evaluated once numerical values of λ_m, $R_m(1)$, and C_m have been obtained for given values of α or $u_s/\bar{u}$.

The Nusselt number may be determined from the definition of a thermal diameter D_T, which depends on the area of the heating surface (ref. 4). For the present analysis, $D_T = 8L/\sigma$. Then, when this definition is applied,

$$Nu \equiv \frac{hD_T}{\kappa} = \frac{q}{t_w - t_b} \frac{8L}{\sigma\kappa}$$

When equation (3~~5~~3) is used,

$$Nu = \frac{4}{G(1) + \frac{\sigma\xi_t}{2L} + \sum_{m=1}^{\infty} C_m R_m(1) \exp\left(\frac{-\sigma^2 \lambda_m \frac{x}{2L}}{RePr}\right)} \tag{36}$$

The longitudinal variation of the local Nusselt number along the duct, equation (36), can likewise be evaluated as soon as numerical values of λ_m, C_m, and $R_m(1)$ have been obtained.

It is of interest to examine the behavior of the Nusselt number at the entrance of the heated section ($x = 0$) and also in the fully developed region ($x \to \infty$). At the entrance,

$$Nu_0 = \frac{4}{G(1) + \frac{\sigma\xi_t}{2L} + \sum_{m=1}^{\infty} C_m R_m(1)}$$

From equation (24), however, setting $\eta = 1$ yields

$$G(1) = - \sum_{m=1}^{\infty} C_m R_m(1)$$

so that

$$Nu_0 = \frac{4}{\frac{\sigma\xi_t}{2L}} \qquad \sigma = 2,1 \tag{37}$$

In the absence of a temperature-jump effect, the local Nusselt number starts with $Nu_0 \to \infty$. With a temperature jump, however, the local Nusselt number commences with a finite value given by equation (37). Thus, one effect of a temperature jump is a lowering of the starting value of the Nusselt number below its infinite continuum value. The effect of the number of heating surfaces enters through the symmetry number σ.

When equation (36) is used, the fully developed Nusselt number is determined as

$$Nu_d = \frac{4}{G(1) + \frac{\sigma\xi_t}{2L}} \qquad \sigma = 2,1 \tag{38}$$

The function $G(1)$ is evaluated from equation (18a) or (18b) by setting $\eta = 1$. The fully developed Nusselt number then becomes for each case

$$Nu_d = \frac{140/17}{1 - \frac{6}{17}\frac{u_s}{\bar{u}} + \frac{2}{51}\left(\frac{u_s}{\bar{u}}\right)^2 + \frac{70}{17}\frac{\xi_t}{2L}} \qquad \sigma = 2 \tag{39a}$$

$$Nu_d = \frac{140/13}{1 - \frac{3}{26}\frac{u_s}{\bar{u}} + \frac{1}{78}\left(\frac{u_s}{\bar{u}}\right)^2 + \frac{35}{13}\frac{\xi_t}{2L}} \qquad \sigma = 1 \tag{39b}$$

In the absence of rarefaction effects, the fully developed Nusselt number $Nu_{d,c}$ has the value $140/17 = 8.23(\sigma = 2)$ or $140/13 = 10.77(\sigma = 1)$. From equation (39a) or (39b), it is clear that the effects of velocity jump $u_s \neq 0$ would tend to increase the Nusselt number, while the temperature jump would act to decrease the Nusselt number. Similar results have been observed in the case of circular-tube slip flow (ref. 8).

Numerical values of the entrance Nusselt number (eq. (37)) have been evaluated as functions of the parameter $\mu\sqrt{R_g t}/2pL$ and related to the mean free path l by the relation (ref. 8) $(\mu\sqrt{R_g t}/2pL) = \sqrt{2/\pi}(l/2L)$. The values are plotted in figure 2. The values for γ and Prandtl number are representative of air and most diatomic gases. Fully developed Nusselt numbers as given by equations (39) have been evaluated as functions of the two parameters $u_s/\bar{u}$ and $\xi_t/2L$ and are plotted in figure 3 in the form of the ratio $Nu_d/Nu_{d,c}$ where $Nu_{d,c}$ is the appropriate fully developed continuum value. For small values of $\xi_t/2L$ the slip velocity increases the Nusselt number above its continuum value, while for large $\xi_t/2L$ the slip velocity has almost no effect. It is noteworthy that the effects of gas rarefaction are more pronounced in the

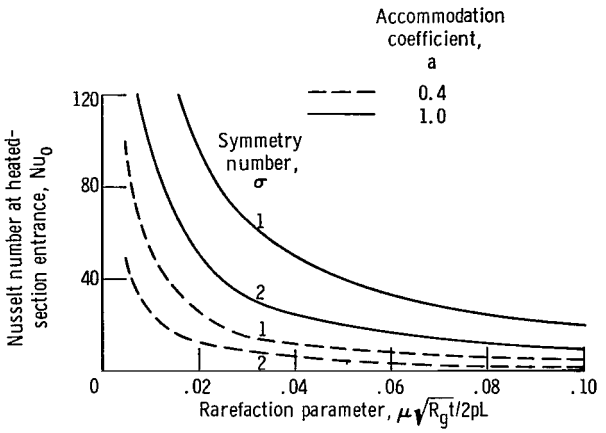

Figure 2. - Effect of gas rarefaction on entrance Nusselt number for parallel-plate channel.

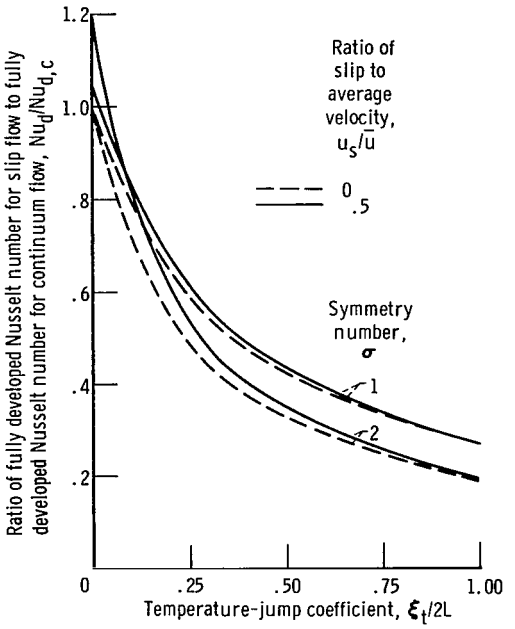

Figure 3. - Fully developed Nusselt numbers for uniform wall heat flux for parallel-plate channel.

case of two-sided heating ($\sigma = 2$) than in the case of one-sided heating ($\sigma = 1$).

It is of interest to present the Nusselt number ratio $Nu_d/Nu_{d,c}$ as a function of the single parameter $\mu\sqrt{R_g t}/2pL$. This is done in figure 4 for $\gamma = 1.4$, $Pr = 0.73$, $g = 1$, and $a = 1.0$ and 0.4. The effect of gas rarefaction is always to decrease the value of the Nusselt number below its continuum value, the result again being more pronounced for two-sided heating than for one-sided heating. Moreover, the differences in results are greater for $a = 0.4$ than for $a = 1.0$.

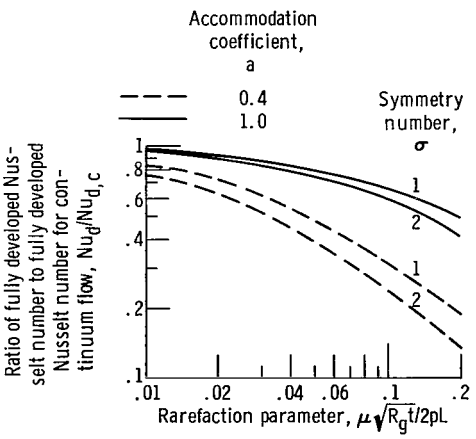

Figure 4. - Fully developed Nusselt number variation in parallel-plate channel with uniform wall heat flux. Specular reflection coefficient, 1; ratio of specific heats, 1.4; Prandtl number, 0.73.

Transverse Distribution Function $R(\eta)$

As mentioned previously, the dimensionless wall-to-bulk temperature difference $(t_w - t_b)/(t_w - t_b)_d$, equation (35), and the local Nusselt number Nu, equation (36), can be evaluated along the entire duct length as soon as the eigenvalues λ_m, eigenfunctions $R_m(\eta)$, and series coefficients C_m have been determined. The function $R_m(\eta)$ is the solution of equation (23):

$$\left.\begin{aligned} &\frac{d^2R}{d\eta^2} + \lambda f(\eta)R = 0 \\ &\frac{dR}{d\eta} = 0 \quad \text{at} \quad \eta = 0 \quad \text{and} \quad \eta = 1 \end{aligned}\right\} \tag{40a}$$

The normalization convention

$$R(0) = 1 \tag{40b}$$

is also used.

For convective heat transfer in laminar continuum flow in a parallel-plate channel with uniform wall heat flux, Sellars, Tribus, and Klein (ref. 1) have obtained asymptotic formulas for the eigenvalues and coefficients through a generalization of constant-wall-temperature results. An improved and more direct treatment of this problem has been given in reference 4. It is of interest to apply the method of reference 1 to laminar flat duct slip flow.

In accordance with the method of reference 1, a solution of the form

$$R(\eta) = \exp[e(\eta)]$$

is considered, where

$$e = \lambda^{1/2}e_0 + e_1 + \frac{e_2}{\lambda^{1/2}} + \ldots$$

and, since λ is assumed to be large, only the first two terms of the previous series are retained (ref. 1). Then it can be shown that the asymptotic solution for $R(\eta)$ is given by

$$R(\eta) = \frac{A \exp\left[i\lambda^{1/2}\int_0^\eta f(\eta)^{1/2}\,d\eta\right] + B \exp\left[-i\lambda^{1/2}\int_0^\eta f(\eta)^{1/2}\,d\eta\right]}{f^{1/4}} \qquad \sigma = 2,1 \tag{41}$$

where A and B are constants to be determined. It should be noted that, for continuum flow ($u_s = 0$), a singularity exists in equation (41) at $\eta = 1$ since $[f(1)]_{\alpha=0} = 0$; this has required the development of an alternate solution, valid near $\eta = 1$ (refs. 1, 4, 6, and 7). For slip flow, no singularity exists at $\eta = 1$ since $[f(1)]_{\alpha\neq 0} = u_s/\bar{u}$ for $\sigma = 2$ and 1. Consequently, equation (41) should be a good approximation over the range $0 \leq \eta \leq 1$ for slip flow, once the constants A and B have been evaluated. As the constants are anticipated to be different for the cases $\sigma = 2$ and $\sigma = 1$, each case will be considered separately.

For the case $\sigma = 2$, the constants A and B are determined from the continuation of equation (41) to the channel central zone $\eta \approx 0$, where $R(\eta)$ can be approximated by the cosine function

$$R(\eta) \approx \cos[(\lambda f(0)^{1/2}\eta] \qquad \eta \approx 0 \tag{42}$$

and thus it is found that to make equations (41) and (42) equal for small η, it is required that

$$A = B = \frac{[f(0)]^{1/4}}{2}$$

so that

$$R(\eta) = \left[\frac{f(0)}{f(\eta)}\right]^{1/4} \cos(\lambda^{1/2} I) \tag{43}$$

where

$$f(\eta) = \frac{3}{2}\,\frac{1 - \eta^2 + 4\alpha}{1 + 6\alpha}$$

$$f(0) = \frac{u_c}{\bar{u}} = \frac{3}{2}\,\frac{1 + 4\alpha}{1 + 6\alpha}$$

$$I \equiv \int_0^{\eta} f(\eta)^{1/2} d\eta = \left(\frac{3}{8}\right)^{1/2} \frac{\left[\eta(1 - \eta^2 + 4\alpha)^{1/2} + (1 + 4\alpha)\arcsin \dfrac{\eta}{(1 + 4\alpha)^{1/2}}\right]}{(1 + 6\alpha)^{1/2}} \tag{44}$$

The slope of $R(\eta)$ at the wall is found by differentiating equation (43) with respect to η and by setting $\eta = 1$. The result is

$$\left(\frac{dR}{d\eta}\right)_{\eta=1} \equiv R'(1) = \frac{1}{2}\,(1 + 4\alpha)^{1/4}(4\alpha)^{-5/4} \cos\left(\lambda^{1/2} I_1\right)$$

$$- \frac{2(4\alpha)^{3/2}\left(\frac{3}{8}\right)^{1/2}\left(\lambda^{1/2} I_1\right)\sin\left(\lambda^{1/2} I_1\right)}{I_1(1 + 6\alpha)^{1/2}} \tag{45}$$

where

$$I_1 \equiv \int_0^1 f(\eta)^{1/2} d\eta = \left(\frac{3}{8}\right)^{1/2} \frac{(4\alpha)^{1/2} + (1 + 4\alpha)\text{arc sin} \dfrac{1}{(1 + 4\alpha)^{1/2}}}{(1 + 6\alpha)^{1/2}} \tag{46}$$

For $R'(1) = 0$, a series of eigenvalues λ_m with the corresponding eigenfunction R_m can be obtained as roots of the characteristic equation

$$\beta_m \tan \beta_m = \frac{(4\alpha)^{1/2} + (1 + 4\alpha)\text{arc sin} \dfrac{1}{(1 + 4\alpha)^{1/2}}}{4(4\alpha)^{3/2}} \equiv E \tag{47}$$

where $\beta_m \equiv \lambda_m^{1/2} I_1$, and E, for a given value of α, is a constant. Tabulated values of the first five roots of equation (47) for a number of values of E are given in reference 10. The values of I_1 for any given slip velocity are shown in figure 5.

To obtain the coefficients C_m (eq. (26)), equation (45) is differentiated with respect to λ, the result is multiplied by λ, and then λ is set equal to λ_m. There is finally obtained

$$\left(\lambda \frac{\partial^2 R}{\partial \eta \, \partial \lambda}\right)_{\eta=1,\, \lambda=\lambda_m} = -\frac{1}{4}(1 + 4\alpha)^{1/4}(4\alpha)^{-5/4}\left(E + 1 + \frac{\beta_m^2}{E}\right)\cos \beta_m \tag{48}$$

Hence,

$$C_m = \frac{1}{\left(\lambda \dfrac{\partial^2 R}{\partial \lambda \, \partial \eta}\right)_{\lambda=\lambda_m,\, \eta=1}} = -4(4\alpha)^{5/4}(1 + 4\alpha)^{-1/4}\left[\left(E + 1 + \frac{\beta_m^2}{E}\right)\cos \beta_m\right]^{-1} \tag{49}$$

When equation (43) and the values $\eta = 1$ and $\lambda = \lambda_m$ are used,

$$R_m(1) = \left(1 + \frac{1}{4\alpha}\right)^{1/4} \cos \beta_m \tag{50}$$

It is convenient to define a new coefficient D_m, given by the product of C_m and $R_m(1)$, as

$$D_m \equiv C_m R_m(1) = -\frac{16\alpha}{E + 1 + \dfrac{\beta_m^2}{E}} \tag{51}$$

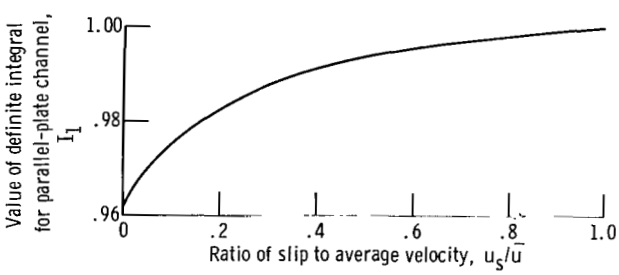

Figure 5. - Value of definite integral for parallel-plate channel for any value of slip to average velocity ratio.

Equations (47) and (51) can be used to calculate the eigenvalues λ_m and coefficients D_m for any given value of α or $u_s/\bar{u}$. In the interests of a unified presentation of results, however, such calculations will be delayed until after the unsymmetrical case $\sigma = 1$ has been treated.

For the unsymmetrical case, the formal asymptotic solution (eq. (41)) is first continued to the insulated wall, $\eta = 0$, where $R(\eta)$ can again be approximated by the cosine function

$$R(\eta) \approx \cos\left\{[\lambda f(0)]^{1/2}\eta\right\} \qquad \eta \approx 0$$

The coefficients A and B are determined to be $A = B = [f(0)]^{1/4}/2$, so that

$$R(\eta) = \left[\frac{f(0)}{f(\eta)}\right]^{1/4} \cos(\lambda^{1/2}\mathcal{S}) \tag{52}$$

where

$$f(\eta) = \frac{6(\eta - \eta^2 + \alpha)}{1 + 6\alpha}$$

$$f(0) = \frac{6\alpha}{1 + 6\alpha} = \frac{u_s}{\bar{u}}$$

and

$$\mathcal{S} \equiv \int_0^\eta f(\eta)^{1/2} d\eta$$

$$= \frac{\left(\frac{3}{8}\right)^{1/2}\left[\alpha^{1/2} + (2\eta - 1)(\eta - \eta^2 + \alpha)^{1/2} - \frac{1}{2}(1 + 4\alpha)\left(\arcsin\frac{1 - 2\eta}{(1 + 4\alpha)^{1/2}} - \arcsin\frac{1}{(1 + 4\alpha)^{1/2}}\right)\right]}{(1 + 6\alpha)^{1/2}} \tag{53}$$

It should be noted that, for continuum flow $\alpha = 0$, equation (5~~3~~2) is not a good approximation to $R(\eta)$ as $\eta \to 0$, since $[f(0)]_{\alpha=0} = 0$, and hence another solution, valid near $\eta = 0$, must be developed (ref. 4). With slip flow no singularity exists at $\eta = 0$.

Continuation to the heated wall $\eta = 1$ results in

$$R(1) = \cos(\lambda^{1/2}\mathcal{S}_1) \tag{54a}$$

$$R'(1) = (4\alpha)^{-1}\left\{\cos\left(\lambda^{1/2}\mathcal{J}_1\right) - \frac{\left[4(\alpha)^{3/2}6^{1/2}\left(\lambda^{1/2}\mathcal{J}_1\right)\sin\left(\lambda^{1/2}\mathcal{J}_1\right)\right]}{\mathcal{J}_1(1 + 6\alpha)^{1/2}}\right\} \tag{54b}$$

where

$$\mathcal{J}_1 \equiv \int_0^1 f(\eta)^{1/2}d\eta$$

$$= \left(\frac{3}{8}\right)^{1/2} \frac{(4\alpha)^{1/2} + (1 + 4\alpha)\text{arc sin}\dfrac{1}{(1 + 4\alpha)^{1/2}}}{(1 + 6\alpha)^{1/2}}$$

$$= I_1 \tag{55}$$

When $R'(1) = 0$, another series of eigenvalues λ_m with the corresponding eigenfunction R_m is obtained as roots of the characteristic equation

$$\beta_m \tan \beta_m = \frac{(4\alpha)^{1/2} + (1 + 4\alpha)\text{arc sin}\dfrac{1}{(1 + 4\alpha)^{1/2}}}{2(4\alpha)^{3/2}}$$

$$\equiv F$$

$$= 2E \tag{56}$$

where now $\beta_m \equiv \lambda_m^{1/2}\mathcal{J}_1 = \lambda_m^{1/2}I_1$.

From the equations developed so far, the coefficients C_m and $D_m \equiv C_mR_m(1)$ are obtained readily as

$$C_m = \frac{1}{\left(\lambda \dfrac{\partial^2 R}{\partial\eta\ \partial\lambda}\right)_{\eta=1,\ \lambda=\lambda_m}} = -8\alpha\left[\left(F + 1 + \frac{\beta_m^2}{F}\right)\cos\ \beta_m\right]^{-1} \tag{57}$$

$$D_m = -\frac{8\alpha}{F + 1 + \dfrac{\beta_m^2}{F}} \tag{58}$$

Equations (47) and (51) for $\sigma = 2$ or equations (56) and (58) for $\sigma = 1$ in conjunction with figure 5 (p. 18) contain all the information essential to the determination of the dimensionless wall-to-bulk temperature variation (eq. (35)) and Nusselt number (eq. (36)) along the entire length of the channels. These

expressions for the pertinent eigenvalues and coefficients are remarkably simple in form and obviously lead to relative ease in computation. It should be recalled that these expressions were derived on the assumption that λ_m is large, and consequently the expressions are supposedly valid only in that limit. The use of these equations for obtaining the first four eigenvalues and coefficients for parametric slip-velocity values of 1/3 and 3/5 yields numerical results that appear to fall between the results for continuum flow $u_s = 0$ and slug flow $u_s/\bar{u} \rightarrow 1$ even for values of m as small as 2. This may be seen from the tabulation and comparison shown in table I(a) for symmetrical two-sided heating $\sigma = 2$, or in table I(b) for unsymmetrical one-sided heating $\sigma = 1$. The results for continuum flow were obtained from expressions presented in reference 4, while for slug flow, the eigenvalues were obtained as the positive roots of $\sin \lambda_m^{1/2} = 0$ or $\lambda_m^{1/2} = m\pi$. The coefficients D_m were obtained from the equally simple result $D_m = -2/\lambda_m$.

The numerical value of 1/3 for $u_s/\bar{u}$ corresponds to $\xi_u/2L = 0.0833$, while a value of 3/5 for $u_s/\bar{u}$ corresponds to $\xi_u/2L = 0.25$. This latter value may perhaps be outside the slip regime. The results for $u_s/\bar{u} = 1$ (slug flow) are definitely outside the slip regime but have been included as limiting values and for comparison.

To check the level of accuracy of the foregoing results, the eigenvalues and eigenfunctions of equation (40a), as well as the coefficients C_m given by equation (25), were computed on an electronic (IBM 7094) computer, by the Runge-Kutta method, for $u_s/\bar{u} = 1/3$ and 3/5. The eigenvalues and coefficients so obtained are listed in table I. The relevant quantities as computed from the previously presented analytical expressions are in remarkably close agreement with the IBM values, especially for values of $m \geq 2$. The fact that the asymptotic formulas give such excellent results for values of m as small as 2 is somewhat surprising. In view of the very good level of agreement that has been demonstrated, it is concluded that the asymptotic formulas are suitable for $m \geq 2$.

The variation of the dimensionless wall-to-bulk temperature difference along the ducts can be evaluated with the numerical information given in table I. Before proceeding with the evaluation, however, it is illuminating to examine the wall-to-bulk temperature difference at the entrance of the heated section. With $x = 0$, equation (35) becomes

$$\frac{(t_w - t_b)_0}{(t_w - t_b)_d} = \frac{G(1) + \dfrac{\sigma\xi_t}{2L} + \displaystyle\sum_{m=1}^{\infty} C_m R_m(1)}{G(1) + \dfrac{\sigma\xi_t}{2L}} \tag{59}$$

When $\eta = 1$, however, equation (24) becomes

$$G(1) = -\sum_{m=1}^{\infty} C_m R_m(1)$$

TABLE I. - EIGENVALUES AND COEFFICIENTS FOR SLIP FLOW IN A PARALLEL-PLATE CHANNEL WITH UNIFORM WALL HEAT FLUX

(a) Symmetry number, 2.

	Ratio of slip to average velocity, $u_s/\bar{u}$					
	0	1/3		3/5		1
		Analytical solution	Numerical solution, Runge-Kutta method	Analytical solution	Numerical solution, Runge-Kutta method	
Eigenvalue						
$\lambda_1^{1/2}$	3.540	3.78	3.33	3.35	3.23	3.14
$\lambda_2^{1/2}$	6.800	6.72	6.49	6.41	6.36	6.28
$\lambda_3^{1/2}$	10.05	9.78	9.65	9.54	9.50	9.42
$\lambda_4^{1/2}$	13.30	12.90	12.82	12.69	12.65	12.56
Coefficient						
D_1	-0.2090	-0.1479	-0.2331	-0.2110	-0.2264	-0.2030
D_2	-.0703	-.0642	-.0701	-.0613	-.0618	-.0508
D_3	-.0367	-.0332	-.0336	-.0282	-.0280	-.0226
D_4	-.0230	-.0198	-.0197	-.0165	-.0161	-.0127

(b) Symmetry number, 1.

	Ratio of slip to average velocity, $u_s/\bar{u}$					
	0	1/3		3/5		1
		Analytical solution	Numerical solution, Runge-Kutta method	Analytical solution	Numerical solution, Runge-Kutta method	
Eigenvalue						
$\lambda_1^{1/2}$	3.800	4.09	3.50	3.51	3.35	3.14
$\lambda_2^{1/2}$	7.071	6.99	6.66	6.51	6.46	6.28
$\lambda_3^{1/2}$	10.33	10.01	9.82	9.61	9.58	9.42
$\lambda_4^{1/2}$	13.60	13.09	12.98	12.72	12.71	12.56
Coefficient						
D_1	-0.1470	-0.0711	-0.1821	-0.1685	-0.1920	-0.2030
D_2	-.0525	-.0425	-.0583	-.0567	-.0566	-.0508
D_3	-.0278	-.0259	-.0291	-.0271	-.0267	-.0226
D_4	-.0176	-.0169	-.0175	-.0156	-.0154	-.0127

so that

$$\frac{(t_w - t_b)_0}{(t_w - t_b)_d} = \frac{\frac{\sigma\xi_t}{2L}}{G(1) + \frac{\sigma\xi_t}{2L}} \tag{60}$$

In the absence of a temperature-jump effect, the wall-to-bulk temperature difference is zero at the entrance. With a temperature jump, however, the entrance temperature difference has a nonzero value. Equation (60) has been plotted in figure 6 as a function of the two parameters $u_s/\bar{u}$ and $\xi_t/2L$ for $\sigma = 2$ and 1. For either wall heating situation the entrance temperature difference increases with an increasing value of $\xi_t/2L$. The magnitude of the slip velocity has only a small influence on the quantity $(t_w - t_b)_0/(t_w - t_b)_d$ for $\sigma = 1$, while for $\sigma = 2$ the influence of slip velocity is more pronounced. It is also seen that rarefaction effects are more strongly exhibited in the two-sided heating than in the one-sided heating situation.

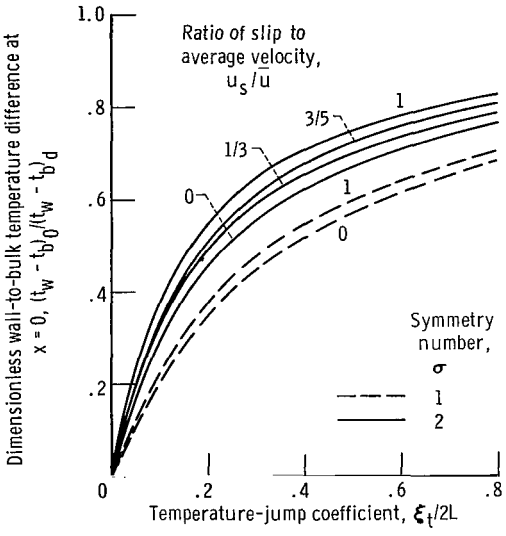

Figure 6. - Variation of dimensionless wall-to-bulk temperature difference at heated section entrance for slip flow in parallel-plate channel with uniform wall heat flux.

The variation of the wall-to-bulk temperature difference along the duct length has been evaluated from equation (35) for several values of the rarefaction parameters $u_s/\bar{u}$ and $\xi_t/2L$. Plots are given in figures 7 and 8 for $\sigma = 2$ and $\sigma = 1$, respectively.

Inspection of figures 7 and 8 reveals several interesting trends. First of all, for a fixed value of $\xi_t/2L$, the wall temperature variation is more sensitive to the slip velocity over most of the duct length for the unsymmetrically heated channel $\sigma = 1$ than for the symmetrically heated channel $\sigma = 2$. Near the entrance, however, the reverse effect is obtained. For both wall heating situations, the slip velocity has the effect of retarding $t_w - t_b$ in its approach to the fully developed value, while the temperature jump has the opposite effect. Finally, it should be noted that the abscissa scale for $\sigma = 1$ is twice that for $\sigma = 2$. Thus, the length required for the wall-to-bulk temperature difference to approach fully developed conditions is greater for the unsymmetrically heated channel than for the channel heated uniformly from both walls.

It is the practice to define a thermal entrance length as the heated length required for $t_w - t_b$ to approach within 5 percent of the fully developed value. A horizontal dashed line corresponding to an ordinate of 0.95 is shown in figures 7 and 8. Then, for example, with $u_s/\bar{u} = \xi_t/2L = 0$, it is

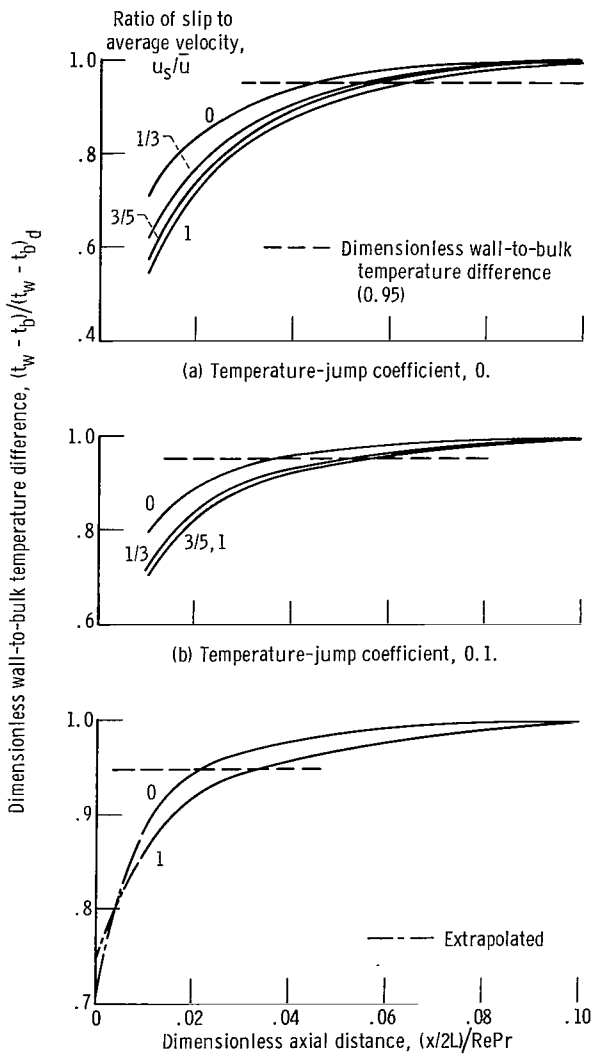

(a) Temperature-jump coefficient, 0.

(b) Temperature-jump coefficient, 0.1.

(c) Temperature-jump coefficient, 0.4.

Figure 7. - Wall temperature ratio in thermal entrance region for flow in parallel-plate channel with uniform wall heat flux and different values of temperature-jump coefficient. Symmetry number, 2.

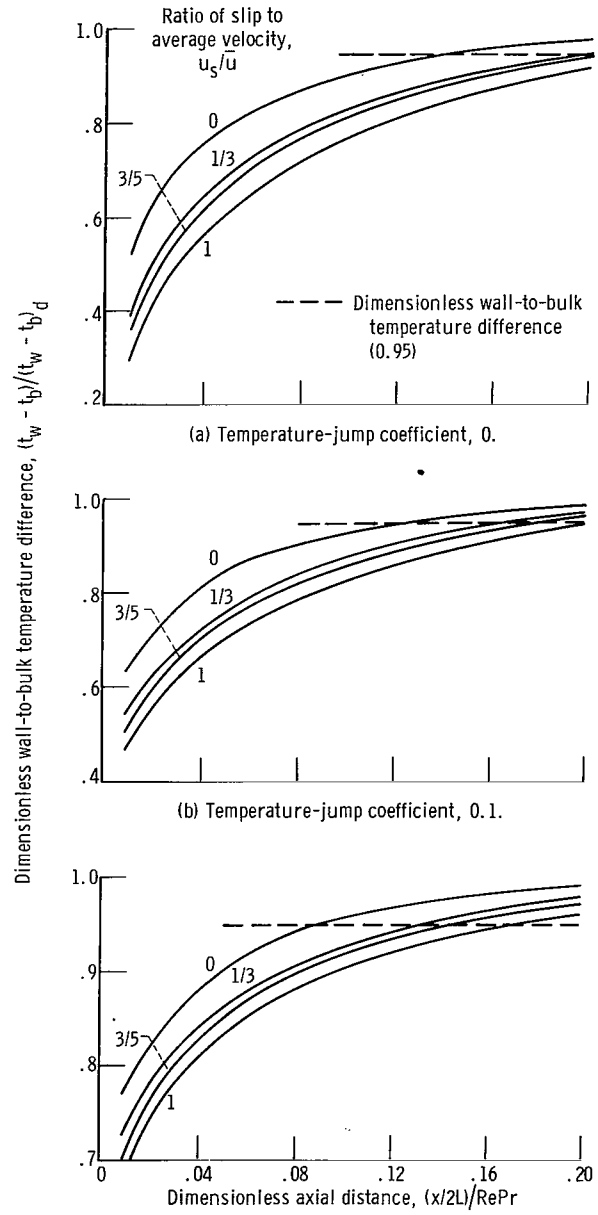

(a) Temperature-jump coefficient, 0.

(b) Temperature-jump coefficient, 0.1.

(c) Temperature-jump coefficient, 0.4.

Figure 8. - Wall temperature ratio in thermal entrance region for flow in parallel-plate channel with uniform wall heat flux and different values of temperature-jump coefficient. Symmetry number, 1.

found that the continuum-flow thermal entrance length is given by $(x/2L)/RePr = 0.045$ ($\sigma = 2$) or 0.144 ($\sigma = 1$). With gas rarefaction the thermal entrance length may shorten, remain the same, or perhaps increase, depending on the relative magnitude of the parameters $u_s/\bar{u}$ and $\xi_t/2L$.

It is perhaps somewhat more illuminating to present the variation of the wall-to-bulk temperature difference in terms of the rarefaction parameter $\mu\sqrt{R_g t}/2pL$. This has been done in figure 9. The effect of increasing gas

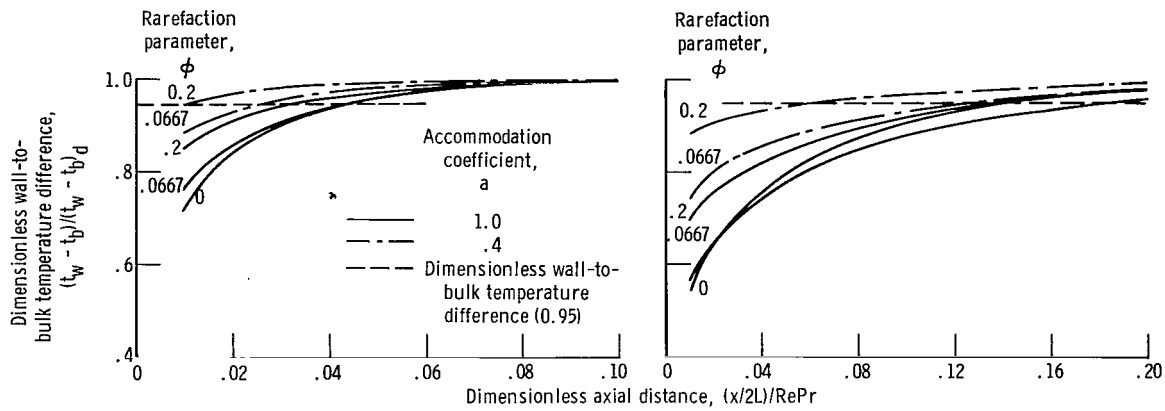

(a) Symmetry number, 2. (b) Symmetry number, 1.

Figure 9. - Wall temperature ratio in thermal entrance region for flow in a parallel-plate channel with uniform wall heat flux. Specular reflection coefficient, 1; ratio of specific heats, 1.4; Prandtl number, 0.73.

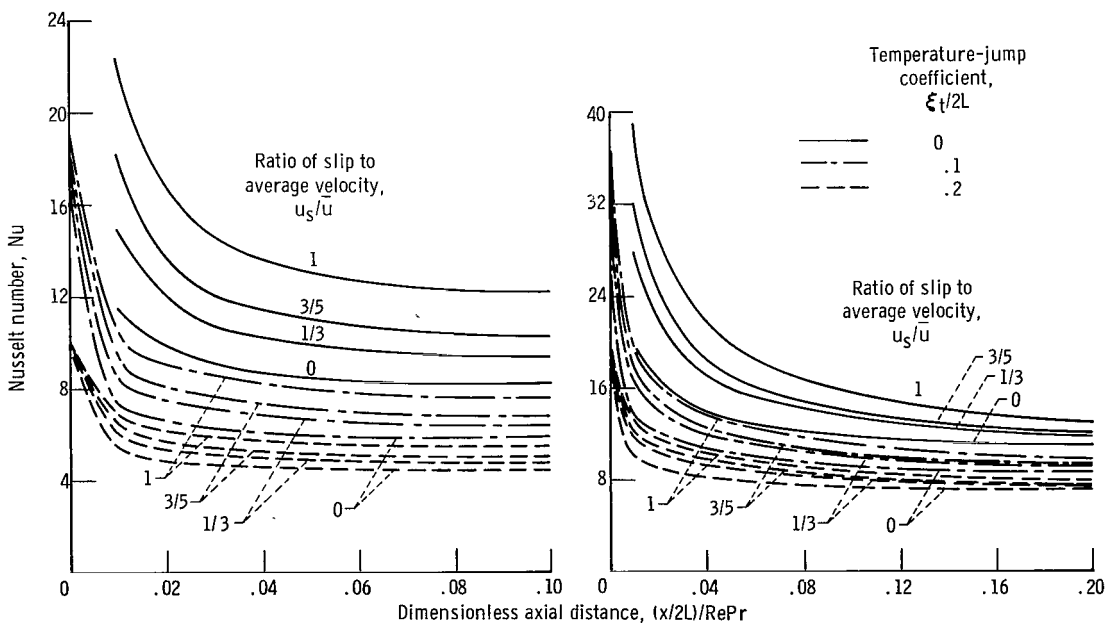

(a) Symmetry number, 2. (b) Symmetry number, 1.

Figure 10. - Variation of Nusselt number along parallel-plate channel for uniform wall heat flux and different values of temperature-jump coefficient.

rarefaction is to shorten the thermal entrance length. The accommodation coefficient also has an important effect on the thermal entrance length, and this is associated with the increase in temperature jump with decreasing accommodation coefficient.

The longitudinal variation of the Nusselt number along the duct with uniform heat flux at one or both walls (eq. (36)) has been evaluated, again by using the data of table I (p. 22) and plotted in figure 10. It is seen that the velocity and temperature jumps give rise to opposite changes in their effect on the Nusselt number variation; the velocity jump tends to increase Nu at a given axial position, while the temperature jump tends to decrease Nu. Numerical evaluations of the Nusselt number dependence on the parameters $\mu\sqrt{R_g t}/2pL$ and a have been plotted in figure 11. Clearly the effect of the

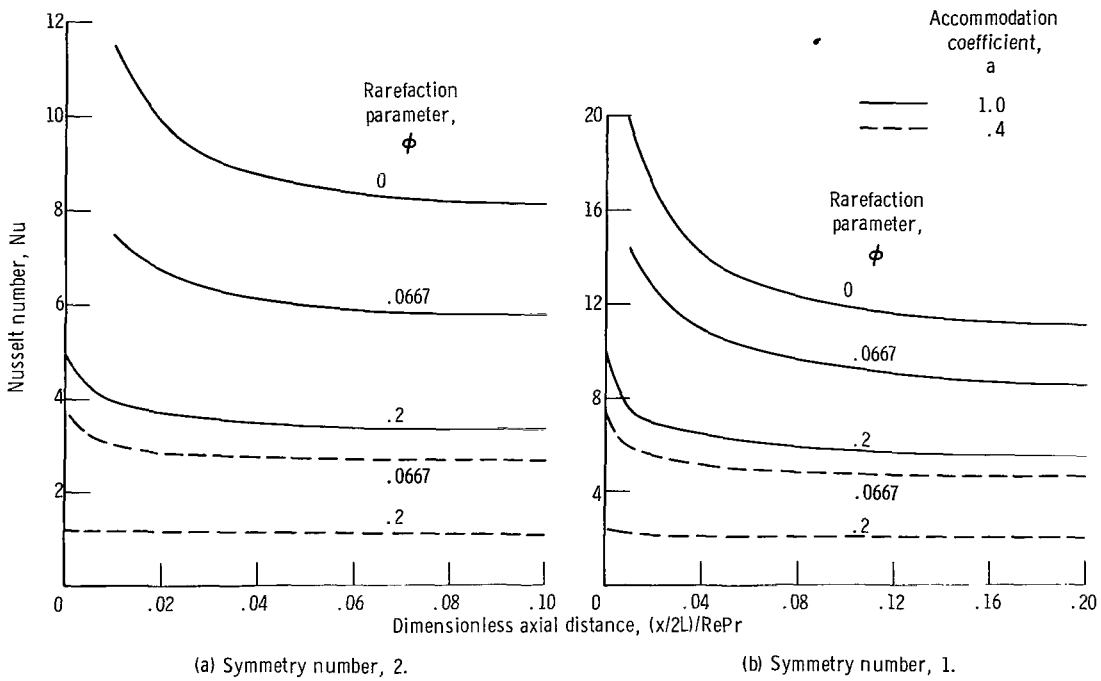

Figure 11. - Variation of Nusselt number along parallel-plate channel for uniform wall heat flux. Specular reflection coefficient, 1; ratio of specific heats, 1.4; Prandtl number, 0.73.

gas rarefaction is always to decrease the Nusselt number below its continuum value at every position along the heated length.

FLOW IN A CIRCULAR TUBE

Attention is now turned to the case of axially symmetric slip flow in a circular tube. The coordinate system for the present problem is shown in figure 12.

It is again assumed that the velocity profile is fully developed and is unchanging along the tube length. The velocity distribution and the fully developed heat-transfer characteristics have already been investigated for the

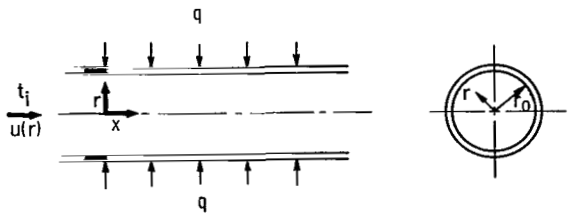

Figure 12. - Physical model and coordinate system for round tube.

circular-tube case (ref. 8) and many results obtained are immediately applicable. The development of the round-tube system is similar to that of the parallel-plate channel. It is, therefore, only necessary to explain the mathematical development in a sketchy way, by discussing the points that differ from the parallel-plate channel case.

The differential equation for convective heat transfer is now

$$\rho C_p u \frac{\partial t}{\partial x} = \frac{\kappa}{r} \frac{\partial}{\partial r} \frac{r\, \partial t}{\partial r} \tag{61}$$

The assumptions and restrictions of this equation are the same as previously explained. When written in terms of the dimensionless variables, equation (61) becomes

$$2\psi f(\omega) \frac{\partial t}{\partial \zeta} = \frac{1}{\omega} \frac{\partial}{\partial \omega} \frac{\omega\, \partial t}{\partial \omega} \tag{62}$$

The velocity distribution u, the slip velocity u_s, and the average velocity $\bar{u}$ have been given in reference 8 as

$$\left.\begin{aligned} u &= -\frac{r_0^2}{4\mu} \frac{dp}{dx} (1 - \omega^2) + u_s \\ u_s &= -\xi_u \left(\frac{du}{dr}\right)_{r=r_0} = -\frac{r_0^2}{\mu} \frac{dp}{dx} \frac{\xi_u}{d} \\ \bar{u} &= -\frac{r_0^2}{8\mu} \frac{dp}{dx} \left(1 + 8 \frac{\xi_u}{d}\right) \end{aligned}\right\} \tag{63}$$

From equation (63) there is easily obtained the dimensionless velocity profile $f(\omega)$ and the slip velocity $u_s/\bar{u}$:

$$f(\omega) = 2 \frac{1 - \omega^2 + 4\alpha}{1 + 8\alpha} \qquad \alpha \equiv \frac{\xi_u}{d} \tag{64}$$

$$\frac{u_s}{\bar{u}} = f(1) = \frac{8\alpha}{1 + 8\alpha} \tag{65}$$

It may readily be shown that for large x a fully developed temperature profile t_d exists in the form

$$\frac{t_d - t_i}{\frac{qr_0}{\kappa}} = \frac{4}{RePr}\frac{x}{r_0} + H(\omega) \tag{66}$$

where the radial function $H(\omega)$ has been given in reference 8 as

$$H(\omega) = \omega^2 - \frac{1}{4}\omega^4 - \frac{7}{24} - \left(\frac{1}{2}\omega^2 - \frac{1}{4}\omega^4\right)\frac{u_s}{\bar{u}} + \frac{1}{24}\left(\frac{u_s}{\bar{u}}\right)^2 \tag{67}$$

The solution for the thermal entrance region can be shown to have the form

$$\frac{t_e}{\frac{qr_0}{\kappa}} = \sum_{n=1}^{\infty} C_n R_n(\omega)\exp\left(\frac{-4\lambda_n \frac{x}{r_0}}{RePr}\right) \tag{68}$$

where λ_n and R_n are, respectively, the eigenvalues and eigenfunctions of the Sturm-Liouville problem:

$$\left.\begin{aligned} &\frac{d}{d\omega}\left(\omega\frac{dR}{d\omega}\right) + 2\lambda\omega f(\omega)R = 0 \\ &\frac{dR}{d\omega} = 0 \qquad \text{at} \qquad \omega = 0,1 \end{aligned}\right\} \tag{69}$$

The coefficients C_n in equation (68) are obtained from the result

$$C_n = \frac{-\int_0^1 2\omega H(\omega)f(\omega)R_n(\omega)d\omega}{\int_0^1 2\omega f(\omega)R_n^2(\omega)d\omega}$$

$$= \frac{\int_0^1 2\omega H(\omega)f(\omega)R_n(\omega)d\omega}{\left[R(\omega)\frac{\partial^2 R}{\partial\omega\,\partial\lambda}\right]_{\omega=1,\,\lambda=\lambda_n}} \tag{70a}$$

or

$$C_n = \frac{1}{\left(\lambda\frac{\partial^2 R}{\partial\omega\,\partial\lambda}\right)_{\omega=1,\,\lambda=\lambda_n}} \tag{70b}$$

To obtain equation (70a), the result

$$H(\omega) = -\sum_{n=1}^{\infty} C_n R_n(\omega) \tag{71}$$

was used. The similarity between equations (70b) and (26) is noteworthy.

The complete solution for the temperature that applies along the entire tube length is obtained by summing equations (66) to (68) to obtain

$$\frac{t - t_i}{\frac{qr_0}{\kappa}} = \frac{4\frac{x}{r_0}}{RePr} + H(\omega) + \sum_{n=1}^{\infty} C_n R_n(\omega)\exp\left(\frac{-4\lambda_n \frac{x}{r_0}}{RePr}\right) \tag{72}$$

The temperature-jump effect at the tube wall is given by

$$t_g - t_w = -2\frac{qr_0}{\kappa}\frac{\xi_t}{d} \tag{73}$$

Hence, the wall temperature along the length of the tube is obtained as

$$\frac{t_w - t_i}{\frac{qr_0}{\kappa}} = \frac{4\frac{x}{r_0}}{RePr} + H(1) + \frac{2\xi_t}{d} + \sum_{n=1}^{\infty} C_n R_n(1)\exp\left(\frac{-4\lambda_n \frac{x}{r_0}}{RePr}\right) \tag{74}$$

This equation can be rephased in terms of the bulk temperature $t_b(x)$ with the result

$$\frac{t_w - t_b}{(t_w - t_b)_d} = \frac{H(1) + \frac{2\xi_t}{d} + \sum_{n=1}^{\infty} C_n R_n(1)\exp\left(\frac{-4\lambda_n \frac{x}{r_0}}{RePr}\right)}{H(1) + \frac{2\xi_t}{d}} \tag{75}$$

where

$$(t_w - t_b)_d = \frac{qr_0}{\kappa}\left[H(1) + \frac{2\xi_t}{d}\right] \tag{76}$$

and

$$t_b(x) = t_i + \frac{\frac{qr_0}{\kappa}\frac{4x}{r_0}}{RePr} \tag{77}$$

The Nusselt number may be determined from the definition

$$Nu \equiv \frac{h(2r_0)}{\kappa} = \frac{q}{t_w - t_b}\frac{2r_0}{\kappa} \tag{78}$$

When equations (76) and (77) are used, the result obtained is

$$Nu = \frac{2}{H(1) + \frac{2\xi_t}{d} + \sum_{n=1}^{\infty} C_n R_n(1)\exp\left(\frac{-4\lambda_n \frac{x}{r_0}}{RePr}\right)} \tag{79}$$

The Nusselt numbers at the entrance of the heated section Nu_0 and in the fully developed region Nu_d are readily obtained from equation (79) as

$$Nu_0 = \frac{1}{\frac{\xi_t}{d}} \tag{80}$$

$$Nu_d = \frac{48/11}{1 - \frac{6}{11}\frac{u_s}{\bar{u}} + \frac{1}{11}\left(\frac{u_s}{\bar{u}}\right)^2 + \frac{48}{11}\frac{\xi_t}{d}} \tag{81}$$

The effect of temperature jump on entrance Nusselt number (eq. (80)) is shown in figure 13. The effects of gas rarefaction on the fully developed Nusselt number (eq. (81)) have been considered in reference 8.

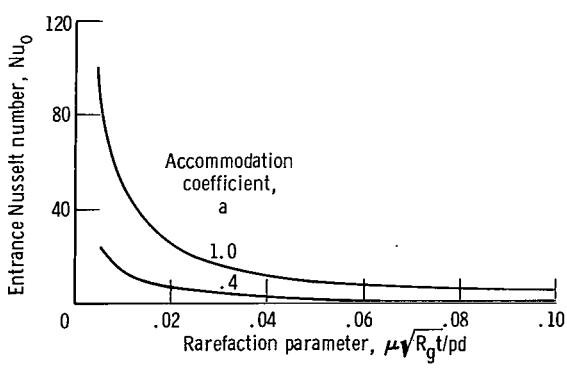

Figure 13. - Effect of gas rarefaction on entrance Nusselt number for a round tube.

The method used to solve the parallel-plate system is completely applicable and can be adopted practically unchanged to determine the asymptotic behavior of equation (69) at large values of λ. By applying this method, it can be shown that the asymptotic solution of equation (69) is given by (ref. 11)

$$R(\omega) = (\pi\omega)^{-1/2}\left(\frac{2}{\lambda f}\right)^{1/4} \cos\left(\lambda^{1/2}\tilde{I} - \frac{\pi}{4}\right) \tag{82}$$

where

$$f(\omega) = 2\,\frac{1 - \omega^2 + 4\alpha}{1 + 8\alpha}$$

$$\tilde{I} \equiv \int_0^{\omega} [2f(\omega)]^{1/2} d\omega = \omega(1 - \omega^2 + 4\alpha)^{1/2} + (1 + 4\alpha)\text{arc sin}\,\frac{\omega}{(1 + 4\alpha)^{1/2}} \tag{83}$$

See Errata

It is noteworthy that for continuum flow equation (82) has a singularity at $\omega = 1$, and, consequently, continuation to the wall zone $\omega = 1$ requires the development of an alternate solution valid near $\omega = 1$ (refs. 1 and ~~13~~. For slip flow, equation (82) is continuous throughout the interval $0 \leq \omega \leq 1$.

The slope of $R(\omega)$ at the tube wall $R'(1)$ is found by differentiating equation (82) with respect to ω, and then by setting $\omega = 1$, which yields

$$R'(1) = \frac{1}{4}\left(\frac{2}{\pi}\right)^{1/2}\left(\frac{1 + 8\alpha}{\lambda}\right)^{1/4}(4\alpha)^{-5/4}\left\{\left[M\left(\lambda^{1/2}\tilde{I}_1\right) + N\right]\cos\left(\lambda^{1/2}\tilde{I}_1\right) + \left[-M\left(\lambda^{1/2}\tilde{I}_1\right) + N\right]\sin\left(\lambda^{1/2}\tilde{I}_1\right)\right\} \tag{84}$$

where

$$\tilde{I}_1 \equiv \int_0^1 [2f(\omega)]^{1/2} d\omega = \frac{(4\alpha)^{1/2} + (1 + 4\alpha)\text{arc sin}\,\dfrac{1}{(1 + 4\alpha)^{1/2}}}{(1 + 8\alpha)^{1/2}} \tag{85}$$

$$M \equiv \frac{4(4\alpha)^{3/2}}{(4\alpha)^{1/2} + (1 + 4\alpha)\text{arc sin}\,\dfrac{1}{(1 + 4\alpha)^{1/2}}} \tag{86}$$

$$N \equiv 1 - 4\alpha \tag{87}$$

Setting $R'(1) = 0$ yields the eigenvalues λ_n as roots of the characteristic equation

$$\tan\beta_n = \frac{M\beta_n + N}{M\beta_n - N} \tag{88}$$

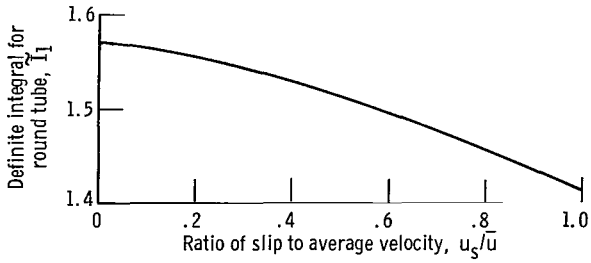

Figure 14. - Values of definite integral for any value of slip to average velocity ratio in round tube.

where $\beta_n \equiv \lambda_n^{1/2}\tilde{I}_1$. The values of $\tilde{I}_1$ for any given slip velocity $u_s/\bar{u}$ are shown in figure 14.

The coefficients of the series expansion (eq. (74)) are

$$D_n \equiv C_n R_n(1) = \frac{-16\alpha}{N + \frac{N^2}{M} + M\beta_n^2} \tag{89}$$

Table II shows the first four eigenvalues and coefficients for the case of flow in a round tube. The results for continuum flow $(u_s/\bar{u} = 0)$ were obtained from expressions given by Dzung (ref. 3), while for slug flow $(u_s/\bar{u} \rightarrow 1)$ the eigenvalues were obtained as the roots of $J_1(2\lambda_n)^{1/2} = 0$, where J_1 is a Bessel function of the first kind and the first order. The coefficients D_n are then obtained from the simple result $D_n = -1/\lambda_n$. Also shown in table II are the data obtained through the use of an IBM 7094 computer by the Runge-Kutta method. It is apparent that the asymptotic formulas yield values of sufficient accuracy for $n \geq 2$.

TABLE II. - EIGENVALUES AND COEFFICIENTS FOR SLIP FLOW IN A CIRCULAR TUBE WITH UNIFORM WALL HEAT FLUX

	Ratio of slip to average velocity, $u_s/\bar{u}$					
	0	2/5		2/3		1
		Analytical solution	Numerical solution, Runge-Kutta method	Analytical solution	Numerical solution, Runge-Kutta method	
Eigenvalue						
$\lambda_1^{1/2}$	2.531	----	2.55	2.64	2.60	2.710
$\lambda_2^{1/2}$	4.578	4.71	4.63	4.75	4.74	4.955
$\lambda_3^{1/2}$	6.599	6.76	6.69	6.88	6.86	7.195
$\lambda_4^{1/2}$	8.610	8.81	8.75	9.00	8.98	9.425
Coefficient						
D_1	-0.1985	----	-0.1855	-0.1670	-0.1658	-0.1360
D_2	-.0693	-0.0594	-.0605	-.0515	-.0510	-.0406
D_3	-.0365	-.0306	-.0301	-.0247	-.0245	-.0194
D_4	-.0230	-.0217	-.0185	-.0145	-.0144	-.0113

The variation of the dimensionless wall-to-bulk temperature difference for a uniform wall heat flux has been evaluated and plotted in figure 15 for the special case $\xi_t/d = 0$ by using the numerical data of table II. Figure 16

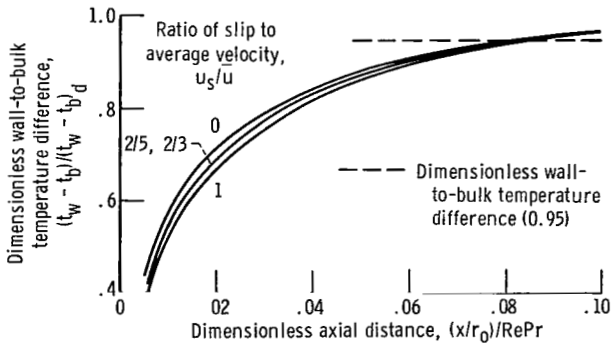

Figure 15. - Wall temperature ratio in thermal entrance region of round tube for uniform wall heat flux and temperature-jump coefficient of zero.

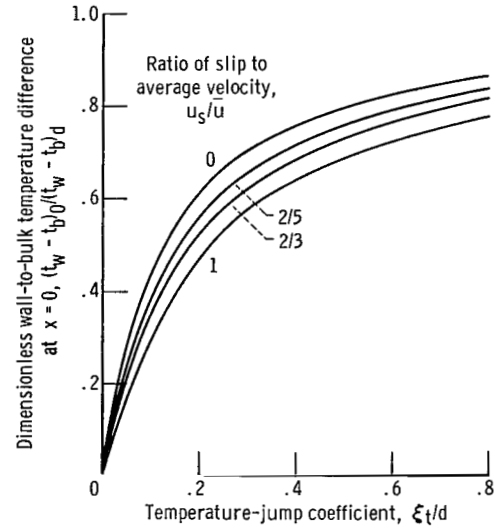

Figure 16. - Variation of dimensionless wall-to-bulk temperature difference at heated section entrance for slip flow in a round tube with uniform wall heat flux.

shows the variations in $(t_w - t_b)_0/(t_w - t_b)_d$ due to gas rarefaction.

Numerical values of the Nusselt number variation along the tube length (eq. (79)) have been evaluated as functions of the two parameters $u_s/\bar{u}$ and ξ_t/d and are plotted in figure 17. The trends are similar to those observed in the parallel-plate channel system. The Nusselt number variation can be cal-

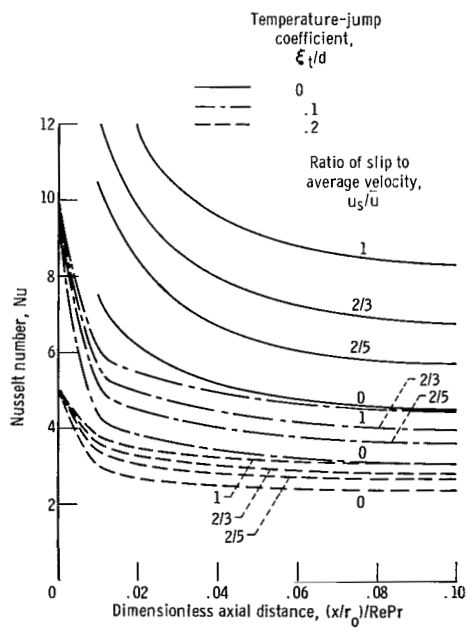

Figure 17. - Variation of Nusselt number along round tube for uniform wall heat flux and different values of temperature-jump coefficient.

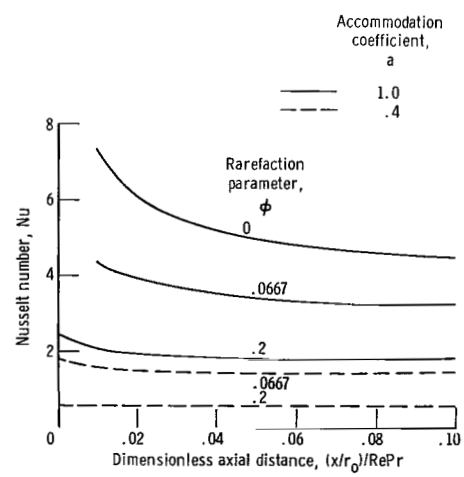

Figure 18. - Variation of Nusselt number along round tube for uniform wall heat flux. Specular reflection coefficient, 1; ratio of specific heats, 1.4; Prandtl number, 0.73.

culated as a function of the parameter $\mu\sqrt{R_g t}/pd$. This has been done, and the results are plotted in figure 18. Increasing gas rarefaction and/or decreasing accommodation coefficient reduces the Nusselt number below its continuum value, and, in addition, shortens the thermal entrance length, which has been defined alternatively as the heated length required for the Nusselt number to approach within 5 percent the fully developed value as given by equation (81).

OTHER RAREFACTION EFFECTS

In reference 8, modification of the fully developed heat-transfer results for laminar tube slip flow is made to account for additional slip effects such as wall shear work, modified temperature jump, and thermal creep velocity. For the sake of completeness, extension of the present more general analyses is made, or discussed, to include these additional slip effects.

Shear Work at the Wall

Maslen in reference 12 proposed that, when there is a slip flow, an energy balance at the wall must include the shear work done by the slipping gas. Analyses given in references 13 and 14 have lent support to this proposal for tube flow, at least when viscous dissipation within the gas is also considered.

If q denotes the heat transfer at the wall, then for the symmetrically heated channel $\sigma = 2$ and for the uniformly heated circular tube, Maslen's proposal is equivalent to writing the temperature derivative at the wall as

$$\left.\begin{aligned} \kappa\left(\frac{\partial t}{\partial y}\right)_{y=L} &= q + q^* \qquad \text{(parallel-plate channel)} \\ \kappa\left(\frac{\partial t}{\partial r}\right)_{r=r_0} &= q + q^* \qquad \text{(circular tube)} \end{aligned}\right\} \tag{90}$$

where q^* is defined in reference 8 as

$$q^* \equiv \frac{\mu u_s^2}{\xi_u} \tag{91}$$

Thus if everywhere q formerly appeared there is now written $q + q^*$, the prior analyses continue to be applicable.

In the case of the channel with unsymmetrical wall heat flux $\sigma = 1$, the temperature derivatives at the wall now become

$$\left.\begin{aligned} \kappa\left(\frac{\partial t}{\partial y}\right)_{y=2L} &= q + q^* \equiv q_1 \\ \kappa\left(\frac{\partial t}{\partial y}\right)_{y=0} &= -q^* \equiv q_2 \end{aligned}\right\} \tag{92}$$

Clearly, the nature of the problem has changed from one in which the upper wall is heated while the lower wall is insulated to one in which the constant heat rates at the upper and the lower walls are q_1 and q_2, respectively, and hence the problem must be reexamined. Such examination will be omitted here. It suffices to say that such an analysis has been given for continuum channel flow (ref. 7), and undoubtedly it can be extended to slip-flow conditions.

Modified Temperature Jump

It has been suggested in reference 15 that the temperature jump derived for a stationary fluid be modified to one for a moving fluid. This proposal is equivalent to altering equations (28) and (73) to read, respectively,

$$t_g - t_w^* = -\xi_t\left(\frac{\partial t}{\partial y}\right)_{y=2L/\sigma} \qquad \text{(parallel-plate channel)} \tag{93a}$$

$$t_g - t_w^* = -\xi_t\left(\frac{\partial t}{\partial r}\right)_{r=r_0} \qquad \text{(circular tube)} \tag{93b}$$

where, from reference 8,

$$t_w^* = t_w + \left(\frac{4\gamma}{\gamma + 1} + \frac{1 - a}{a}\,\frac{g}{2 - g}\right)\left(\frac{u_s^2}{c_p}\right) \tag{94}$$

Thus, if t_w is replaced by t_w^* at all places, the prior analyses continue to be applicable.

The foregoing analysis assumes zero shear work at the walls. In the event of nonzero shear work, it can be shown for the symmetrically heated channel $\sigma = 2$ and for the circular tube that equations (93) must be altered to read

$$t_g - t_w^* = -\xi_t\,\frac{q + q^*}{\kappa} \tag{95}$$

Therefore, the previously derived results continue to apply. For the channel with the lower wall insulated ($\sigma = 1$), the boundary condition becomes

$$t_g - t_w^* = -\xi_t\,\frac{q + q^*}{\kappa}$$

at the upper wall, and

$$t_g - t_w^* = \frac{\xi_t q^*}{\kappa} \tag{96}$$

at the lower wall. Thus, the problem is now one of unsymmetrically prescribed gas temperatures adjacent to the walls. Such a boundary condition has been considered in reference 2 for continuum flow, and undoubtedly the results can

be modified to cover the present slip-flow problem.

Thermal Creep

When a gas adjacent to a surface encounters a temperature gradient along the surface, there will be an additional velocity (thermal creep) induced in the direction of increasing temperature (ref. 16). Equations (2) and (3) must be altered to read, respectively,

$$u_s = \pm\xi_u\left(\frac{\partial u}{\partial y}\right)_{y=\mp L} + \frac{3}{4}\frac{\mu R_g}{p}\left(\frac{\partial t}{\partial x}\right)_{y=\mp L} \tag{97a}$$

$$u_s = \pm\xi_u\left(\frac{\partial u}{\partial y}\right)_{y=\left|\begin{smallmatrix}0\\2L\end{smallmatrix}\right.} + \frac{3}{4}\frac{\mu R_g}{p}\left(\frac{\partial t}{\partial x}\right)_{y=\left|\begin{smallmatrix}0\\2L\end{smallmatrix}\right.} \tag{97b}$$

for the parallel-plate channel system, while for the circular tube the slip velocity is given by

$$u_s = -\xi_u\left(\frac{\partial u}{\partial r}\right)_{r=r_0} + \frac{3}{4}\frac{\mu R_g}{p}\left(\frac{\partial t}{\partial x}\right)_{r=r_0} \tag{97c}$$

The analyses in the earlier sections have not included the thermal creep velocity. As a consequence, the velocity field could be determined independently of the temperature and treated as fully developed. The temperature field, however, is a function of the velocity (eqs. (10) and (61)). If thermal creep is not negligible, the temperature and velocity fields are mutually interdependent, and then a fully developed velocity distribution can be achieved only for the condition where $\partial t/\partial x$ is a constant. An examination of equation (27) for the parallel-plate channel system, or equation (72) for the circular tube system, shows that $\partial t/\partial x$ is a constant in that portion of the conduit where the fully developed heat-transfer condition is attained. In the thermal entrance region $\partial t/\partial x$ varies with x. The coupled momentum and energy equations might be solved by successive approximations with the thermal creep velocity assumed small, but not negligible. Perhaps another approach would be to seek a similarity variable such that the temperature and velocity fields can be described by a single space variable. The problem would then be reduced to a system of ordinary differential equations that may be amenable to analytical or numerical solutions.

In any event, the present solutions without the inclusion of thermal creep are still very useful as they represent the zero-order solution and the first step toward the solution of the more complicated situation that exists when the phenomenon of thermal creep is considered. In addition, it is believed that

the present solutions have led to a better general understanding of the laminar heat-transfer characteristics in conduits under slip-flow conditions.

Lewis Research Center
National Aeronautics and Space Administration
Cleveland, Ohio, March 13, 1964

REFERENCES

1. Sellars, J. R., Tribus, M., and Klein, J. S.: Heat Transfer to Laminar Flow in a Round Tube or Flat Conduit - The Graetz Problem Extended. Trans. ASME, vol. 78, no. 2, Feb. 1956, pp. 441-448.

2. Cess, R. D., and Shaffer, E. C.: Summary of Laminar Heat Transfer Between Parallel Plates with Unsymmetrical Wall Temperatures. Jour. Aero. Sci., vol. 26, no. 8, Aug. 1959, p. 538.

3. Dzung, L. S.: Heat Transfer in a Round Duct with a Sinusoidal Heat Flux Distribution. Proc. Second U.N. Conf. on Peaceful Uses of Atomic Energy (Geneva), vol. 7, 1958, pp. 657-670.

4. Dzung, L. S.: Heat Transfer in a Flat Duct with Sinusoidal Heat Flux Distribution. Proc. Second U.N. Conf. on Peaceful Uses of Atomic Energy (Geneva), vol. 7, 1958, p. 671-675.

5. Siegel, R., Sparrow, E. M., and Hallman, T. M.: Steady Laminar Heat Transfer in a Circular Tube with Prescribed Wall Heat Flux. Appl. Sci. Res., Sec. A, vol. 7, 1958, pp. 386-392.

6. Cess, R. D., and Shaffer, E. C.: Heat Transfer to Laminar Flow Between Parallel Plates with a Prescribed Wall Heat Flux. Appl. Sci. Res., Sec. A, vol. 8, 1959, pp. 339-344.

7. Cess, R. D., and Shaffer, E. C.: Laminar Heat Transfer Between Parallel Plates with an Unsymmetrically Prescribed Heat Flux at the Walls. Appl. Sci. Res., Sec. A, vol. 9, 1959, pp. 64-70.

8. Sparrow, E. M., and Lin, S. H.: Laminar Heat Transfer in Tubes under Slip-Flow Conditions. Jour. Heat Trans., vol. 84, no. 4, Nov. 1962, pp. 363-369.

9. Chambré, P. L., and Schaaf, S. A.: Flow of Rarefied Gases. Princeton Univ. Press, 1961.

10. Carslaw, H. S., and Jaeger, J. C.: Conduction of Heat in Solids. Oxford University Press, 1959, p. 491.

11. Inman, R. M.: Approximation of the Eigenvalues for Heat Transfer in Laminar Tube Slip Flow. AIAA Jour., Feb. 1964.

12. Maslen, S. H.: On Heat Transfer in Slip Flow. Jour. Aero. Sci., vol. 25, no. 6, June 1958, pp. 400-401.

13. Inman, R. M.: Consideration of Energy Separation for Laminar Slip Flow in a Circular Tube. Jour. Aero. Sci., vol. 29, no. 8, Aug. 1962, pp. 1014-1015.

14. Inman, R. M.: Energy Separation in Laminar Vortex-Type Slip Flow. AIAA Jour., vol. 1, no. 6, June 1963, pp. 1411-1412.

15. Oman, R. A., and Scheuing, R. A.: On Slip-Flow Heat Transfer to a Flat Plate. Jour. Aero. Sci., vol. 26, no. 2, Feb. 1959, pp. 126-127.

16. Kennard, E. H.: Kinetic Theory of Gases. McGraw-Hill Book Co., Inc., 1938, p. 327.

NASA-Langley, 1964 E-2431

= 17/2
02

"The aeronautical and space activities of the United States shall be conducted so as to contribute . . . to the expansion of human knowledge of phenomena in the atmosphere and space. The Administration shall provide for the widest practicable and appropriate dissemination of information concerning its activities and the results thereof."

—NATIONAL AERONAUTICS AND SPACE ACT OF 1958

NASA SCIENTIFIC AND TECHNICAL PUBLICATIONS

TECHNICAL REPORTS: Scientific and technical information considered important, complete, and a lasting contribution to existing knowledge.

TECHNICAL NOTES: Information less broad in scope but nevertheless of importance as a contribution to existing knowledge.

TECHNICAL MEMORANDUMS: Information receiving limited distribution because of preliminary data, security classification, or other reasons.

CONTRACTOR REPORTS: Technical information generated in connection with a NASA contract or grant and released under NASA auspices.

TECHNICAL TRANSLATIONS: Information published in a foreign language considered to merit NASA distribution in English.

TECHNICAL REPRINTS: Information derived from NASA activities and initially published in the form of journal articles.

SPECIAL PUBLICATIONS: Information derived from or of value to NASA activities but not necessarily reporting the results of individual NASA-programmed scientific efforts. Publications include conference proceedings, monographs, data compilations, handbooks, sourcebooks, and special bibliographies.

Details on the availability of these publications may be obtained from:

SCIENTIFIC AND TECHNICAL INFORMATION DIVISION

NATIONAL AERONAUTICS AND SPACE ADMINISTRATION

Washington, D.C. 20546